University of Zurich[UZH]

Zurich Open Repository and Archive
University of Zurich
Main Library
Strickhofstrasse 39
CH-8057 Zurich
www.zora.uzh.ch

Year: 2013

Analysis of the uniaxial and multiaxial mechanical response of a tissue-engineered vascular graft

Mauri, Arabella; Zeisberger, Steffen M; Hoerstrup, Simon P; Mazza, Edoardo

Abstract: Tissue engineering is aimed at the fabrication of autologous cardiovascular implants, for example, heart valves or vascular grafts. To date, the mechanical characterization of tissue-engineered vascular grafts (TEVGs) has focused mainly on the material's strength and not on the deformation behavior. A total of 31 samples obtained from 3 mature grafts (out of the cells of a single donor) were tested in uniaxial stress and uniaxial strain configurations to characterize their stiffness under uniaxial and biaxial stress states, respectively. Corresponding measurements were carried out on samples of an ovine artery. A physiological stiffness parameter was defined for data analysis and the uniaxial and multiaxial response compared, also in terms of anisotropy. The tension-strain curve of uniaxial stress tests is highly nonlinear, whereas the results show a more gradual deformation response of the material under a uniaxial strain configuration, which better represents the physiological state of biaxial stress. Stiffness parameters and anisotropy factors are significantly influenced by the selection of the testing configuration. Tangent stiffness of a TEVG at physiological loading conditions is significantly ($p<0.05$) higher for uniaxial stress as compared to uniaxial strain. The same is observed for the ovine tissue. The anisotropy of the scaffold is shown to partially transfer to the mature TEVG. The results of this study show that for a TEVG characterization, a physiological biaxial testing configuration should be preferred to the commonly used uniaxial stress.

DOI: https://doi.org/10.1089/ten.tea.2012.0075

Posted at the Zurich Open Repository and Archive, University of Zurich
ZORA URL: https://doi.org/10.5167/uzh-72705
Journal Article
Published Version

Originally published at:
Mauri, Arabella; Zeisberger, Steffen M; Hoerstrup, Simon P; Mazza, Edoardo (2013). Analysis of the uniaxial and multiaxial mechanical response of a tissue-engineered vascular graft. Tissue Engineering. Part A, 19(5-6):583-592.
DOI: https://doi.org/10.1089/ten.tea.2012.0075

TISSUE ENGINEERING: Part A
Volume 19, Numbers 5 and 6, 2013
© Mary Ann Liebert, Inc.
DOI: 10.1089/ten.tea.2012.0075

Original Article

Analysis of the Uniaxial and Multiaxial Mechanical Response of a Tissue-Engineered Vascular Graft

Arabella Mauri, MSc,[1] Steffen M. Zeisberger, PhD,[2,3]
Simon P. Hoerstrup, PhD,[2,3] and Edoardo Mazza, PhD[1,4]

Tissue engineering is aimed at the fabrication of autologous cardiovascular implants, for example, heart valves or vascular grafts. To date, the mechanical characterization of tissue-engineered vascular grafts (TEVGs) has focused mainly on the material's strength and not on the deformation behavior. A total of 31 samples obtained from 3 mature grafts (out of the cells of a single donor) were tested in uniaxial stress and uniaxial strain configurations to characterize their stiffness under uniaxial and biaxial stress states, respectively. Corresponding measurements were carried out on samples of an ovine artery. A physiological stiffness parameter was defined for data analysis and the uniaxial and multiaxial response compared, also in terms of anisotropy. The tension–strain curve of uniaxial stress tests is highly nonlinear, whereas the results show a more gradual deformation response of the material under a uniaxial strain configuration, which better represents the physiological state of biaxial stress. Stiffness parameters and anisotropy factors are significantly influenced by the selection of the testing configuration. Tangent stiffness of a TEVG at physiological loading conditions is significantly ($p < 0.05$) higher for uniaxial stress as compared to uniaxial strain. The same is observed for the ovine tissue. The anisotropy of the scaffold is shown to partially transfer to the mature TEVG. The results of this study show that for a TEVG characterization, a physiological biaxial testing configuration should be preferred to the commonly used uniaxial stress.

Introduction

Many strategies have been applied in recent years to overcome the lack of viable autologous replacement materials for the repair of congenital cardiovascular malformations, as the currently used prostheses are associated with adverse side-effects. Tissue engineering may have the potential to overcome disadvantages, such as life-long anticoagulation therapy, increased risks for reoperation, and thromboembolism.[1–4] The scientific effort of the last two decades has resulted in a fast development of tissue-engineered vascular grafts (TEVGs), leading to clinical trials in humans with a positive long-term outcomes.[5] To optimize the compatibility of TEVGs after implantation, different scaffold materials[6–8] and various cell sources[9–12] have been investigated and are the focus of prospective developments.

The importance of mechanical stimulation on the tissue development during the production of TEVGs is recognized.[11,13–15] Also, problems related to compliance mismatch between engineered and native tissues are well-known in artificial prostheses.[16] Nevertheless, the assessment of the deformation behavior of these grafts is often rudimentary, no standard protocols exist, nor criteria for data analysis. More work was done to determine the strength of the tissue-engineered vessels and many researchers analyzed the rupture behavior of the grafts under internal pressure. Similar attention should also be given to the deformation behavior, which determines the performance and mechanical biocompatibility of TEVGs. In Table 1, the mechanical properties of TEVGs based on the polyglycolic acid (PGA) nonwoven mesh are reported. The scaffold material has to be considered when comparing TEVGs, because its structure influences the mechanical response of the mature graft. As can be seen, little information is given on the nonlinear tensile response, and the data comes short of determining the multiaxial, anisotropic deformation behavior of TEVGs. Available information is limited to uniaxial stress tensile tests, prevalently in the longitudinal direction, and to inflation to burst tests. A description of the deformation behavior of TEVGs in the physiological loading range—both in circumferential and longitudinal directions—is needed to compare their mechanical characteristics with those of the tissue they are intended to

[1]Department of Mechanical and Process Engineering, ETH Zurich, Zurich, Switzerland.
[2]Swiss Center for Regenerative Medicine (SCRM), University Hospital Zurich and University of Zurich, Zurich, Switzerland.
[3]Department of Surgical Research and Clinic for Cardiovascular Surgery, University Hospital Zurich, Zurich, Switzerland.
[4]Swiss Federal Laboratories for Materials Science and Technology, EMPA, Duebendorf, Switzerland.

Table 1. Mechanical Properties of TEVGs Based on PGA Nonwoven Mesh Reported as Mean ± Standard Deviation

	Scaffold	*Cell source*	*Weeks*			*Reference*
Tensile modulus				Circumferential	Longitudinal	
[MPa]	PGA-P4HB	HVSM	4	-	2.3 ± 0.57^{a}	[38]
	PGA-P4HB	HVSM	3	-	$2.64 \pm 0.47^{a,b}$	[39]
	PGA + PCL + PGA	BA	2	3.75 ± 0.78^{a}	-	[40]
	PGA-P4HB	HVSM	4 (FBS)	-	3.94 ± 2.02^{a}	[41]
	PGA-P4HB		4 (PL)	-	1.33 ± 0.90^{a}	[41]
				Pulsatile	Static	
Burst pressure	PGA	PCA	7–8	803 ± 105	-	[42]
[mmHg]	PGA-P4HB	OCA	1	177.5 ± 10	178.8 ± 4	[13]
			2	240.0 ± 28	110.0 ± 18	
			3	262.5 ± 26	90.0 ± 8	
			4	326.3 ± 24	50.0 ± 5	
	3 PGA layers	BA	5	570 ± 100	-	[43]
			8	2150 ± 709	-	

[a]Slope of the linear region (tangent modulus corresponding to E_{high}).
[b]0% of prestrain.
TEVGs, tissue-engineered vascular grafts; PGA, polyglycolic acid; FBS, fetal bovine serum; PL, platelet-lysate; HVSM, human *vena saphena magna*; OJV, ovine jugular vein; OCA, ovine carotid artery; PCA, porcine carotid artery; BA, bovine aorta.

substitute. Substantial progress has been achieved in recent years for the experimental characterization of the multiaxial response of soft biological tissues.[17,18] However, a planar biaxial testing set-up is expensive and not available in most laboratories. Another limitation of this configuration is related to the boundary conditions, which are difficult to control, in particular, for small samples.[19–20]

In the present work, we investigate the mechanical properties of a human TEVG and of a native ovine tissue under uniaxial and biaxial stress states. The latter is achieved using the so called pure shear or uniaxial strain configuration.[21] The uniaxial strain test is easy to perform and induces a biaxial state of stress in the tissue, which more closely represents the physiological conditions of TEVG loading. The experiments were carried out using an experimental set-up similar to the one proposed by Hollenstein *et al.*[22] Tissue-engineered material had not been characterized under the uniaxial strain configuration before. Herein, a physiologically relevant method is proposed to evaluate the stiffness and the anisotropy of these tissues.

Material and Methods

Tissue-engineered vascular graft

Cell isolation, expansion, and seeding have been done as previously described by Hoerstrup *et al.*[2,4] All procedures were conducted after informed consent of the donor, according to institutional guidelines of the University Hospital Zurich and the ethics committee of the Kanton Zurich, Switzerland (Permission Nr. 21/2006).

Bioabsorbable scaffolds were fabricated from nonwoven polyglycolic-acid mesh (PGA, thickness 1.0 mm, specific gravity 70–90 mg/cm^3, Cellon SA) coated with poly-4-hydroxybutyrate (P4HB, molecular weight 1×10^6, PHA 4400, Tepha Inc.). Based on biopsies of human peripheral blood vessels, endothelial cells (ECs) were obtained using a collagenase-instillation technique. Following isolation, they were cultured in tissue culture flasks (Nunc™) with an endothelial basal medium (EBM-2) supplemented with 10% FBS (GIBCO). To obtain myofibroblasts (MFs), the remaining de-endothelialized vessel segments were minced and cultured in the Dulbecco's modified Eagle's Medium (DMEM; GIBCO) supplemented with 10% FBS and 2 mM glutaMAX (GIBCO). After MFs migration onto the dishes (after 5–7 days), cells were serially passaged and expanded in a humidified incubator at 37°C and 5% CO_2. Sufficient cell numbers for cell seeding were obtained in pure culture after 10–14 days.

MFs ($4.5–5.5 \times 10^6/cm^2$) were sequentially seeded onto the vascular scaffolds, followed by EC seeding ($1 \times 10^6/cm^2$) phenotypically confirmed by the von Willebrand Factor (vWF) presence. Thereafter, the constructs were transferred into a pulse duplicator system[2] and grown under gradually increasing nutrient medium flow conditions (50–550 mL/min, 1 Hz) for 14 days. Media were changed every 3–4 days. A total of 31 samples were gained from 3 mature grafts (ca. 10 samples from each graft) out of the same patient's cells. The TEVG samples had a thickness of approximately 1.5 mm. Scaffold samples were prepared using PGA meshes with P4HB coating.

Ovine tissue

The sheep is an established animal model in cardiovascular surgery, because blood pressure is representative for the human system, the dimensions of the arteries are comparable (but typically larger in humans) and normal tissue is available. Moreover, the implants are exposed to higher calcification than in a human body defining this environment as the worst case. In the past, TEVGs (developed with ovine cells) have been successfully implanted in an ovine pulmonary artery[4] and in the future, these grafts might be used as aortic implants.

The native ovine tissue samples were collected from six proximal descending thoracic aortas (sample thickness ~2.5 mm) and three pulmonary arteries (sample thickness ~3 mm) obtained directly from the slaughterhouse. The

material was held in a physiological saline solution and tested within 48 h. Vessels were cut in the axial direction and opened up to generate longitudinal and circumferential samples. Regions near to bifurcations with smaller arteries were excluded from the testing material.

Testing protocol

Small sample dimensions were chosen to cover all the experimental configurations (uniaxial stress and uniaxial strain) and directions (circumferential and longitudinal). The samples were collected in the circumferential and in the longitudinal direction to assess the material's anisotropy. Samples for uniaxial stress tests (Fig. 1a) were cut with a special tool composed of razor blades separated by 2-mm spacers. Samples for uniaxial strain tests (Fig. 1b) were cut with a surgical scalpel.

The number of samples tested for the relevant materials in each configuration is reported in Figure 1. Note that the area of the cut samples (including the clamped part) changes substantially between the addressed configurations. Since the same amount of the TEVG tissue was used for each testing configuration, the number of obtained samples is lower for uniaxial strain ($n=6$) compared to uniaxial stress ($n=25$).

Figure 1 displays the fundamental differences of uniaxial stress (on top) and of uniaxial strain (below) configurations. The uniaxial stress configuration does not constrain the lateral contraction of the material, generating a multiaxial deformation. The resulting stress state is uniaxial, that is, stress vectors in the material are oriented in the direction of elongation. On the contrary, the uniaxial strain configuration has a large clamping width, which constrains the lateral contraction and induces a transversal stress. Therefore, this configuration generates in the plane of the membrane a state of uniaxial deformation and biaxial stress. Since TEVGs and arteries are subjected to blood pressure-induced stress in circumferential as well as longitudinal directions, the uniaxial strain test better represents physiological loading conditions.

Tissue-engineered and native materials were tested with a custom-made tensile machine controlled with LabView (National Instruments). The testing set-up includes a linear horizontal motor (PI M-505 4PD; Physik Instrumente GmbH) and a 10 N load cell (KAW-S, AST Mess- und Regelungstechnik). A video extensometer with a telecentric objective is placed on top of the experimental set-up and records images with a frequency of 1 Hz. During experiments, force and displacement were sampled at 17 Hz. To produce

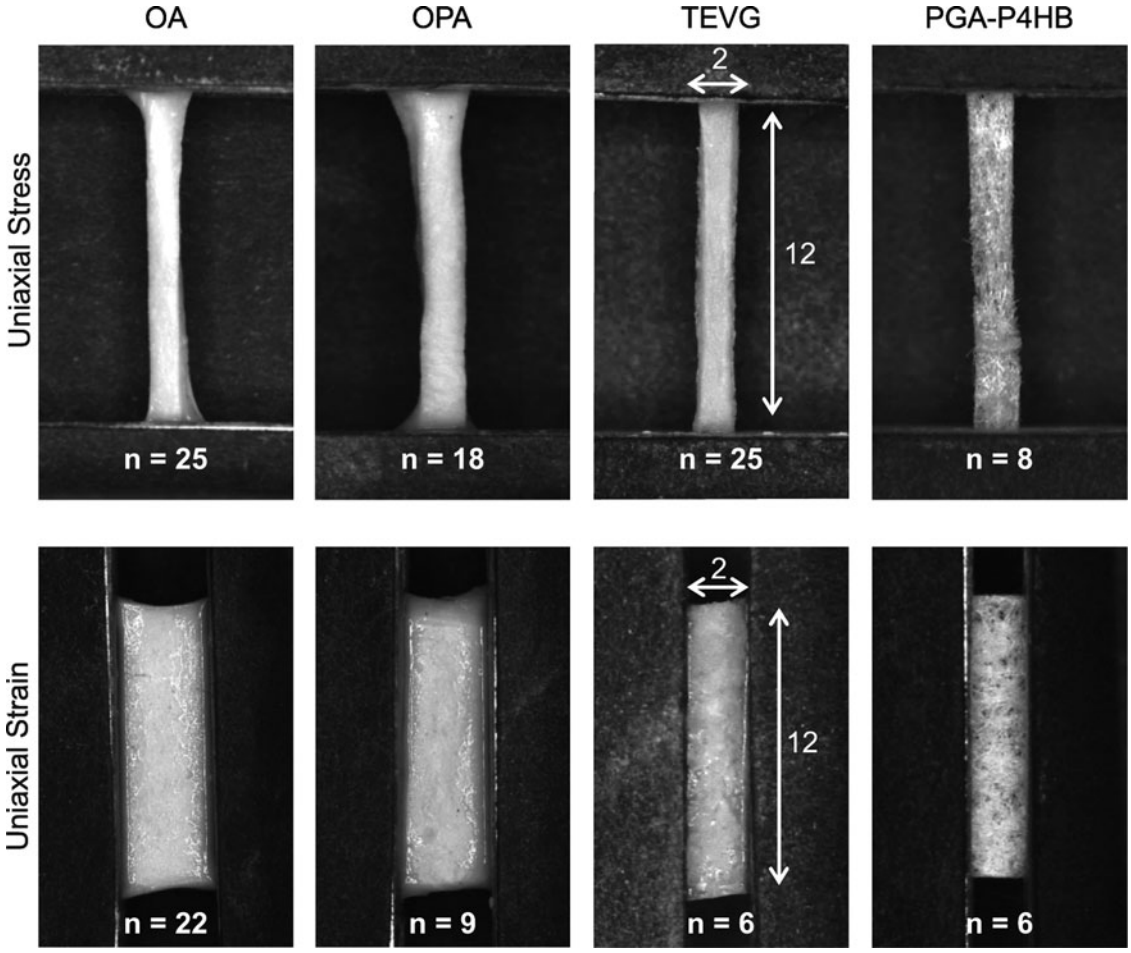

FIG. 1. Overview of the tested material in configuration of uniaxial stress and uniaxial strain. The material and number of samples (n) are indicated under a representative picture of the clamped sample. Initial sample dimensions [mm] are indicated in the example of the TEVG specimens. OA, ovine aorta; OPA, ovine pulmonary artery; TEVG, tissue-engineered vascular graft; PGA-P4HB: PGAscaffold with P4HB coating.

comparable results, the same sample geometry and testing protocol were used for scaffold, tissue-engineered, and ovine native material. The protocol consists of 10 cycles preconditioning at 10% of nominal strain and successively of one ramp until 50% nominal strain for TE material or until 200% nominal strain for native tissue. For the latter, a larger amount of nominal strain had to be applied to achieve the required tension range. All samples were tested with a constant strain rate of 1%/s. The duration of each experiment never exceeded 10 min, so that significant dehydration of the samples can be excluded.

Analysis of the experimental data

The aim of mechanical characterization was to determine the structural properties of TEVGs as membranes, rather than the material properties. Thus, the deformation response is reported as nominal tension over nominal strain. The nominal tension is defined as force over the sample width. The nominal strain corresponds to the difference between the current and the initial length divided by the latter. The choice of considering values of tension instead of stress was primarily given by the fact that TEVGs are to be evaluated and compared with the native tissue in terms of their structural response, rather than the local material response. The width of each specimen was calculated out of the image of the clamped sample in the initial configuration.

The definition of one scalar stiffness parameter, such as Young's modulus for linear elastic materials, is difficult for biological tissues, due to their pronounced nonlinearity. Instead of characterizing the initial and final slope of the J-shaped tension–elongation curve, we chose a tangent modulus TM at the physiological load. This scalar parameter describes the deformation response of the material near to its relevant loading state. For this purpose, an estimation of the physiological tension in the aorta and in the pulmonary artery was carried out under the assumption of a thin-walled vessel. The physiological tension was estimated in circumferential T_{circ} and in longitudinal T_{long} direction as:

$$T = p \cdot R \cdot A \tag{1}$$

where p is the internal mean blood pressure, R is the vessel's radius and A is equal to 1 for T_{circ} or 0.5 for T_{long}. However, to assess the anisotropy of the tissues, the stiffness parameter needs to be evaluated at the same tension value for both directions. Therefore, a T_{physio} was defined as the mean of T_{circ} and T_{long}. Average p and R values for ovine arteries were used in this calculation, since the ovine tissue was selected for comparison in this study. Corresponding values for human arteries are slightly higher, due to larger vessel diameters. Tension values of 100 and 19 mN/mm were obtained as T_{physio} for the ovine aorta and ovine pulmonary artery, respectively. As shown in Figure 2d, a region of the tension–strain curve centered at the selected tension level is linearized and the corresponding slope determined, leading to the tangent modulus TM. Statistical analysis to assess differences between groups was performed using the Wilcoxon rank-sum test. A p-value < 0.05 was considered significant.

Results

The deformation properties of the considered tissues membrane were measured in uniaxial stress and in uniaxial strain configurations. This approach allows quantifying

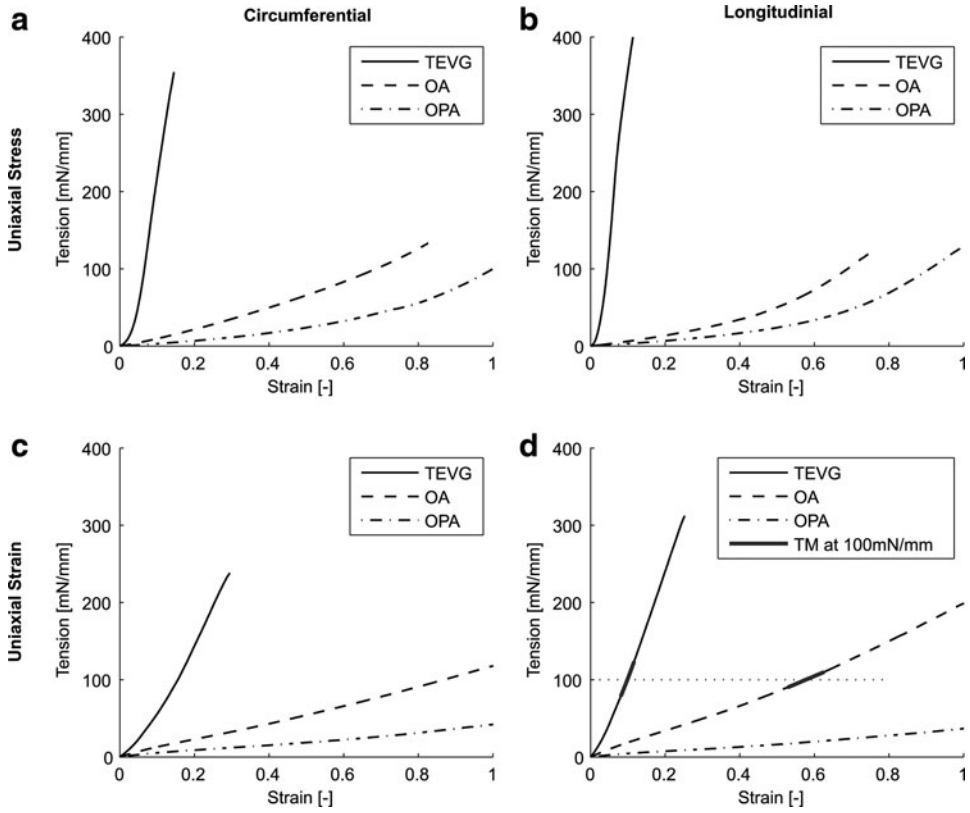

FIG. 2. Deformation behavior of a human TEVG (full line), ovine aortic tissues (broken line) and of pulmonary arteries (dashed line) are plotted. Results are reported in terms of nominal tension (force divided by initial width) and strain (current divided by initial length minus one). The experimental results are shown for uniaxial stress in circumferential **(a)** and in longitudinal **(b)** directions. The result of the more physiological uniaxial strain configuration is reported for the circumferential **(c)** and the longitudinal **(d)** direction. The curve region considered for determination of the tangent modulus TM is shown as an example in **(d)** for TEVG and ovine aorta.

differences in the material response under the uniaxial or biaxial stress state. The mean tension–stretch curve of TEVG samples, the mean ovine–aorta curve and the mean ovine–pulmonary artery curve are represented in Figure 2. The results for the uniaxial stress configuration are displayed in circumferential (a) and longitudinal (b) directions. These curves show a significant nonlinearity at increasing tensions. The results for the uniaxial strain configuration are reported in circumferential (c) and longitudinal (d) directions. In this biaxial stress state, the material response for small deformation is comparable to the one at larger loading levels, for the TEVG as well as for the native tissue.

In the last graph (d), the region of the curve used for determining the tangent modulus is highlighted for the example of 100 mN/mm tension on the TEVG and the ovine aorta. As previously defined, the tangential stiffness parameters TM of the TEVG are evaluated at two different physiological tension levels, 100 and 19 mN/mm, corresponding, respectively, to the aorta and pulmonary artery expected mean physiological loading. Tangential moduli obtained in uniaxial stress and uniaxial strain configurations for TE and the native tissue are displayed in Figure 3. The variability of the results among three grafts is within the standard deviation of the single graft. Therefore, all the TEVG samples are considered as a single group. Despite the variability of results typical of biological materials, the effect of the testing configurations on the deformation response results are significant ($p < 0.05$) for all materials and in both directions (numerical values reported in Table 3).

The mechanical response is stiffer in the uniaxial stress configuration for all tested materials, when compared to uniaxial strain. For the TEVG configuration, the stiffness increases to a factor larger than 2, whereas, for the ovine native tissue, this factor is of approximately 1.5. TEVGs are stiffer than the ovine native tissue, but the difference is much lower if the materials are compared under a uniaxial strain configuration.

The anisotropy of the tissue is represented with the mean anisotropy factor, which is defined as TM_{circ}/TM_{long} of the different tissues (numerical values reported in Table 4). These factors are reported for the ovine native tissues and the human TEVG at the physiological tensions of 100 and 19 mN/mm. Additionally, the scaffold material is reported for the example of 100 mN/mm. It can be seen that the TEVG and the aortic tissue show larger (significant) anisotropy in the uniaxial stress as compared to the uniaxial strain configuration. The TEVG and the ovine artery have the same anisotropy direction (a stiffer longitudinal response). Instead, for the pulmonary artery, the anisotropy factor is near to one (i.e., a quasi-isotropic response). The same trend can be seen for the scaffold material: (1) PGA-P4HB is stiffer in the longitudinal direction and (2) the anisotropy factor is larger in the uniaxial stress configuration than in the uniaxial strain configuration.

Discussion

The present study focuses on the deformation behavior of a TEVG in a physiological range of mechanical loading. However, the data also provide information to evaluate the tissue reserve before rupture. During the uniaxial stress tests, TEVG samples achieved (circumferential) tension values at

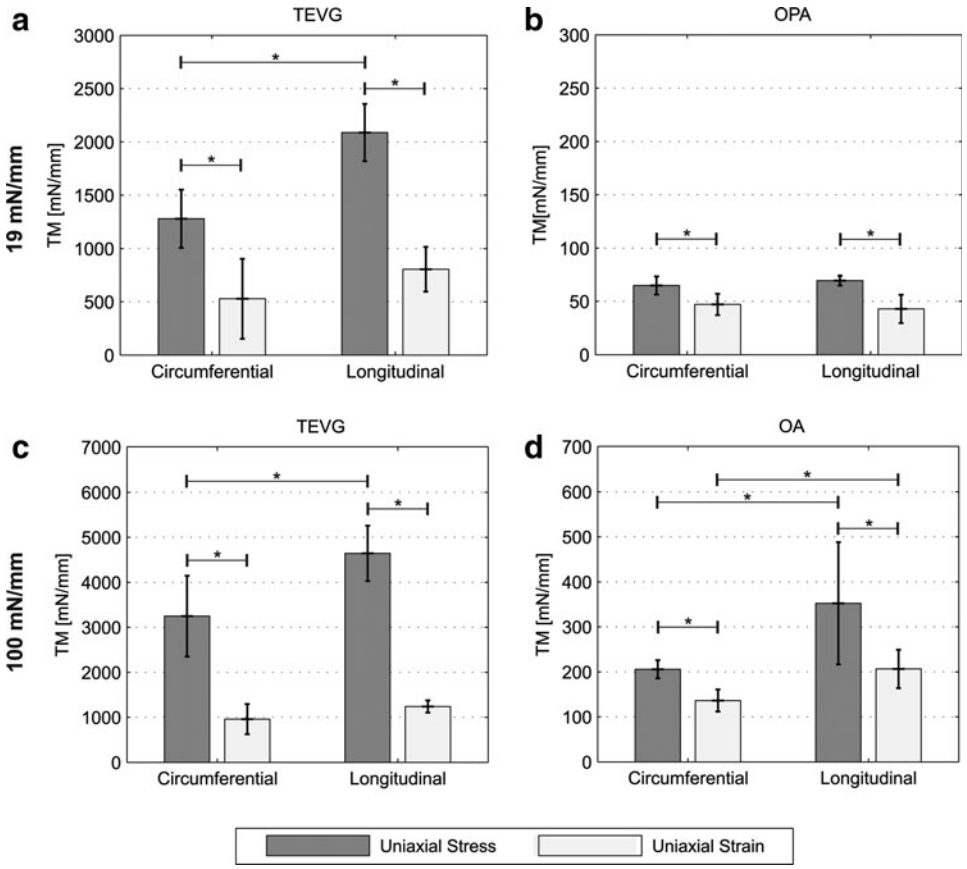

FIG. 3. The stiffness parameters of a human TEVG, OPA, and OA are reported in circumferential and longitudinal directions. The stiffness moduli TMi are evaluated at the physiological tension loading of 19 mN/mm **(a, b)** and of 100 mN/mm **(c, d)**.

Table 2. Mechanical Properties of Native Tissue are Reported as Mean ± Standard Deviation in the Respective Testing Direction (Circumferential and Longitudinal)

	Material	*Ultimate stress [MPa]*		*Tensile modulus [MPa]*		*Reference*
Tensile test		Circ	Long	Circ	Long	
	H DTA	1.76 ± 0.22	1.96 ± 0.6	2.42 ± 0.56[a]	1.55 ± 0.44[a]	[29]
	B A	0.88 ± 0.13	-	3.31 ± 0.56[b]	-	[40]
	P CA	-	Nr	-	10 ± 7[b]	[26]
	H DTA	1.72 ± 0.89	1.47 ± 0.91	-	-	[44]
	P DTA	-	1.15 ± 0.39	-	2.98 ± 1.45[b]	[45]
	H AA	-	1.21 ± 0.33	-	5.69 ± 1.38[c]	[46]
	H ATA	1.80 ± 0.24	1.71 ± 0.14	3.25 ± 0.63[c]	2.61 ± 0.26[c]	[27]

	Material	*Burst pressure [mmHg]*	*Stiffness modulus[d] [MPa]*		*Reference*
Inflation to Burst			Circ	Long	
	H EIA and *SFA*	nr	1.271[e]	-	[47]
	P common CA	3323 ± 413	45.1 ± 16.8[f]	-	[42]
	H DTA	nr	11.4 ± 8.9[b]	-	[28]
	H internal *MA*	3196 ± 1264	-	-	[48]
	H SV	1599 ± 877	-	-	[48]
	H SV	1680 ± 307	-	-	[49]
	H internal MA	4225 ± 1368	-	-	[50]

[a]Secant modulus at rupture.
[b]Slope of the linear region (tangent modulus corresponding to E_2).
[c]Maximum slope prior to failure.
[d]Approximated nominal stress-strain curves were evaluated in each test and analyzed to determine a stiffness modulus.
[e]Tangential modulus calculated at 100 mmHg.
[f]Tangential modulus as slope of the four highest values of strain before failure.
H, human; *O*, ovine; *P*, porcine; *B*, bovine; *AA*, abdominal aorta; *ATA*, ascending thoracic aorta; *DTA*, descending thoracic aorta; *CoA*, coronary artery; *CA*, carotid artery; *IA*, iliofemoral artery; *MA*, mammary artery; *PA*, pulmonary artery; *EIA*, external iliac artery; *SFA*, femoral artery; *SV*, saphenous vein; nr, not reported.

rupture above 350 mN/mm. This tension is 3.5 times larger than the physiological value for the ovine aorta and 18.4 times larger for the pulmonary artery. It should be noted that the uniaxial stress configuration does not correspond to the physiological condition of loading and deformation, and leads to internal material reorganization, possibly with significant rearrangement of fiber's orientation. The uniaxial strain configuration is considered as more representative for evaluation of an *in vivo* mechanical performance. In this configuration, the samples achieved (circumferential) tensions above 240 mN/mm without rupture, generating a corresponding reserve factor larger than 2.4 and of 12.6 for the aorta and pulmonary artery, respectively. For this reason and based on the ovine model system, the TEVG is confirmed to safely withstand the *in vivo* situation.

A suitable scalar parameter has to be defined to compare the curves representing the deformation behavior of the different materials. The characterization of a material through the formulation of continuum model equations is more comprehensive, but complex; see, for example, Ehret *et al.*[23] Such models are necessary to predict the full three-dimensional material response under different loading states. However, a well-chosen scalar parameter is sufficient for the purpose of the present work, to compare the stiffness of different tissues in a specific, physiologically relevant range of mechanical loading.

Table 3. The Deformation Behavior of the TEVG is Compared to the Material Response of Ovine Aorta and Ovine Pulmonary Artery at the Physiological Tension of 100 mN/mm and 19 mN/mm, Respectively

	Configuration		*TM_{TEVG} [mN/mm]*	*TM_i [mN/mm]*
19 mN/mm OPA	Circumferential	UA Stress	1279 ± 273	65 ± 8
		UA Strain	528 ± 375	47 ± 10
	Longitudinal	UA Stress	2087 ± 268	69 ± 5
		UA Strain	805 ± 211	43 ± 13
100 mN/mm OA	Circumferential	UA Stress	3246 ± 899	206 ± 20
		UA Strain	960 ± 336	136 ± 24
	Longitudinal	UA Stress	4643 ± 616	352 ± 136
		UA Strain	1240 ± 135	207 ± 43

Tangent moduli (TM) are reported as mean ± standard deviation for uniaxial stress and uniaxial strain configurations in longitudinal and circumferential directions.
OA, ovine aorta; OPA, ovine pulmonary artery; UA, uniaxial.

Table 4. The Mean Anisotropy Factor (MAF) is Defined as TM_{CIRC}/TM_{LONG}

	19 mN/mm		*100 mN/mm*		
Configuration	MAF_{TEVG} [−]	MAF_{OPA} [−]	MAF_{OA} [−]	MAF_{TEVG} [−]	$MAF_{PGA\text{-}P4HB}$ [−]
UA Stress	0.61	0.93	0.58	0.70	0.31
UA Strain	0.66	1.09	0.66	0.77	0.60

These factors are evaluated at the physiological tension values of 19 mN/mm for the ovine pulmonary arteries and of 100 mN/mm for the ovine aortas. The scaffold anisotropy is evaluated for the example of 100 mN/mm. The MAFs are reported for uniaxial stress and uniaxial strain configurations.

OA, ovine aorta; OPA, ovine pulmonary artery; TEVG, tissue-engineered vascular graft; PGA-P4HB, PGA scaffold with P4HB coating; UA, uniaxial.

In literature, different stiffness parameters can be found describing the tensile response of the vascular tissue. In uniaxial tests, the deformation curve of the vascular tissue can be approximated by two quasi-linear regions and a nonlinear elbow in the middle. Therefore, most authors describe the material stiffness with the slope of the quasi-linear regions measured in a tensile test. The initial material response is represented by the low strain modulus E_1, whereas the response in the second quasi-linear region is described with the higher strain modulus E_2.[24–27] Similarly, Groenink *et al.*[28] defined two tangential moduli, $E_{elastin}$ and $E_{collagen}$, since they considered the initial stiffness (E_1) as purely a response of the elastin, and the stiffness of the second region (E_2) as a superposed reaction of elastin and collagen. Other groups define the stiffness of the material with a secant modulus at rupture[29] or at a given value of strain.[30,31]

Various stiffness parameters evaluated from inflation to burst tests are also reported in the literature. These parameters are based on model assumptions, which provide a good approximation of the complex stress–strain fields of the physical experiment, in particular, for small (infinitesimal) deformations. The main uncertainty concerns the level of longitudinal strains that is not directly measured nor properly controlled in burst experiments. For this reason, the deformation behavior of the material is not well characterized with this testing configuration. The uniaxial strain configuration proposed in this work leads to stress vectors in the direction of elongation with magnitude, approximately, two times the one of the stress vector in the perpendicular direction (with constrained lateral contraction). This factor of two corresponds to the expected ratio between circumferential and longitudinal loading in the blood vessel, see equation 1. In this sense, the uniaxial strain experiment with elongation in the circumferential direction best represents physiological conditions of mechanical loading.

To investigate the stiffness of the tissue-engineered and native vascular tissues, we chose a tangent modulus evaluated at the physiological tension value. This definition was selected because the physiological situation corresponds to a tension controlled (as opposed to deformation controlled) mechanical problem. In fact, loading results from the internal blood pressure. A tangent modulus was considered instead of a secant modulus for two reasons, (1) the tangent modulus describes the material response in the neighborhood of the physiological tension and, therefore, can represent well the *in vivo* mechanical response; (2) the possible horizontal shift of the curves associated with the definition of the initial reference configuration (determined by the test set-up and protocol) has much less influence on the tangent modulus than on the secant modulus. It should be noted that the reference configuration is also affected by the preconditioning protocol and might differ considerably in the two test configurations (uniaxial stress and uniaxial strain).

Our results for the TEVG are in general agreement with the stiffness parameters found in the literature for comparable materials, see Table 1. The stiffness parameter of the TEVG evaluated with uniaxial stress at 100 mN/mm was converted in MPa under the (realistic) assumption of a thickness of 1.5 mm. In this case, E^{tg}_{long} correspond to 3.09 MPa and E^{tg}_{circ} to 2.17 MPa. The difference in the definition of these parameters and the ones reported in literature should be considered.

The mechanical response of the materials differs considerably between uniaxial stress and uniaxial strain configurations, as can be observed in the tension–stretch curves reported in Figure 2. In the uniaxial strain configuration, the material is loaded in a physiological biaxial stress state, which generates a stable progressive increase of tension with deformation. Indeed, the deformation curves show an immediate initial response of the material and are less nonlinear at higher strains as compared to uniaxial stress curves. These differences in the mechanical response may be related to an internal fiber rearrangement under the uniaxial stress state. Reorientation of fibers is an important factor in the deformation response of the native tissue and was investigated by different groups.[32–36] In the uniaxial stress configuration, due to free lateral contraction, the fibers are free to realign in the loading direction, creating a nonphysiological additional stiffening effect for high tension. This phenomenon explains also why the material response under the uniaxial stress configuration consistently leads to higher stiffness values than the one under the uniaxial strain configuration, which is in contrast with the expectation for linear elastic isotropic and homogeneous materials.

The anisotropy of the TEVG was assessed with both testing configurations and for two tension values (100 and 19 mN/mm). As reported in Table 4, the grafts showed a tendency to be stiffer in the longitudinal direction (significant only for the uniaxial stress configuration). The same anisotropy direction can be found in the PGA-P4HB scaffold, which is still present in the mature grafts. The anisotropy of the TEVG is expected to depend on the PGA-P4HB scaffold material anisotropy and/or the orientation of the biological tissue components in the pulsatile bioreactor. In fact, a larger compliance is consistently observed in the graft as well as in the ovine aorta in the circumferential direction, for both

testing configurations. This might be related to a more pronounced pulsatile deformation in the circumferential direction for these tissues at a loading level comparable to physiological conditions. In the longitudinal direction, larger stiffness of the material is important to avoid overstretch of vessels.

The anisotropy of the native vascular tissue depends on the anatomical region, as first reported by Cox.[37] Indeed, the native ovine aorta shows a clear anisotropy with a stiff longitudinal direction, while the ovine pulmonary artery seems to be isotropic. These results indicate an advantageous match in the stiffness direction between the TEVG and the native ovine aorta.

Due to the importance of the ovine model system (see section 2), it is relevant to compare the deformation behavior of the TEVGs with the ovine tissue. TEVGs are significantly stiffer than the ovine native tissue, especially for the pulmonary artery. The present data demonstrate that the differences between the tissue-engineered and native tissue is less pronounced, if the deformation response is considered at a physiological level of tension in a biaxial state of stress (uniaxial strain configuration), see Table 3.

The human aorta is considerably stiffer when compared with the corresponding ovine tissue (Table 2), so that the difference between compliance of native and engineered tissue is expected to be significantly overestimated in a comparison with ovine arteries. Future benchmark for optimization of the mechanical properties of TEVGs should be obtained through an artery-specific quantitative evaluation based on uniaxial strain experiments on human tissue. However, it is difficult to acquire a sufficient amount of representative healthy native human tissue for comprehensive characterization of the mechanical response.

The proposed protocol for mechanical characterization provides useful insights into the multiaxial deformation behavior of a TEVG and native tissue. The main limitations of the proposed experiments concern (1) the preconditioning protocol and (2) the control of environmental conditions during mechanical testing. (1) The mechanical parameters reported in this article were obtained after application of a preconditioning protocol involving 10 cycles between 0% and 10% of nominal strain in each experiment. This means that not all of the evaluated physiological loading ranges were covered by the preconditioning procedure. Tangent moduli are expected to be affected by preconditioning, although to a much lesser extent for uniaxial strain than for uniaxial stress configurations. Future protocols should include preconditioning over the whole physiological loading range. (2) Experiments should be performed in a liquid environment with the samples immersed in a physiological saline solution at 37°C. This was not the case in the present study. This omission might generate a (small) difference in the absolute value of the material stiffness, thus not significantly affecting the relative comparison of the material response in the two different testing configurations and directions.

The applied strain rate is low as compared to the physiological rate of deformation. The present results are, therefore, considered representative of the long-term response of the material. Future studies should include evaluation of time dependency in the deformation behavior of the TEVG. Future work should also consider the variability in multiaxial stiffness between TEVGs obtained from cells of different donors.

Conclusions

The TEVG and the ovine native tissue have been tested under the uniaxial stress and uniaxial strain configuration, in both the circumferential and the longitudinal directions. A physiological stiffness parameter has been defined to evaluate and compare the mechanical performance of TEVGs and of corresponding native tissues. The TEVG and the ovine aorta showed a stiffer longitudinal direction. The ovine pulmonary artery was found to have a quasi-isotropic response.

The tangential modulus is significantly ($p < 0.05$) higher under the uniaxial stress configuration for all the analyzed tissues (TEVG, OA, and OPA) and in both directions (circumferential and longitudinal). Therefore, to assess the deformation behavior of a biological tissue, a physiologically relevant biaxial testing configuration should be preferred to conventional uniaxial tensile tests, which might induce internal nonphysiological fibers rearrangement.

Acknowledgments

The authors are grateful to the Swiss National Science Foundation (SNSF) for financial support (Project number: 205321-134803/1). The authors would like to thank Rene Stenger (XELTIS AG, Zurich, Switzerland) for providing human TEVGs as test-material. S.P.H. is scientific advisor to XELTIS AG.

Disclosure Statement

No competing financial interests exist.

References

1. Shinoka, T., Breuer, C.K., Tanel, R.E., Zund, G., Miura, T., Ma, P.X., *et al.* Tissue engineering heart valves: valve leaflet replacement study in a lamb model. Ann Thorac Surg **60,** S513, 1995.
2. Hoerstrup, S.P., Sodian, R., Daebritz, S., Wang, J., Bacha, E.A., Martin, D.P., *et al.* Functional living trileaflet heart valves grown *in vitro*. Circulation **102,** III44, 2000.
3. Sutherland, F.W.H., Perry, T.E., Yu, Y., Sherwood, M.C., Rabkin, E., Masuda, Y., *et al.* From stem cells to viable autologous semilunar heart valve. Circulation **111,** 2783, 2005.
4. Hoerstrup, S.P., Cummings, M.R.C.S. I., Lachat, M., Schoen, F.J., Jenni, R., Leschka, S., *et al.* Functional growth in tissue-engineered living, vascular grafts. Circulation **114,** I159, 2006.
5. Hibino, N., McGillicuddy, E., Matsumura, G., Ichihara, Y., Naito, Y., Breuer, C., *et al.* Late-term results of tissue-engineered vascular grafts in humans. J Thorac Cardiovasc Surg **139,** 431, 2010.
6. Yang, S., Leong, K.F., Du, Z., and Chua, C.K. The design of scaffolds for use in tissue engineering. Part I. Traditional factors. Tissue Eng **7,** 679, 2001.
7. Shin, H., Jo, S., and Mikos, A.G. Biomimetic materials for tissue engineering. Biomaterials **24,** 4353, 2003.
8. Pankajakshan, D., and Agrawal, D.K. Scaffolds in tissue engineering of blood vessels. Can J Physiol Pharmacol **88,** 855, 2010.
9. Hibino, N., Shinoka. T., Matsumura, G., Ikada, Y., and Kurosawa, H. The tissue-engineered vascular graft using bone marrow without culture. J Thorac Cardiovasc Surg **129,** 1064, 2005.

10. Mirensky, T.L., Hibino, N., Sawh-Martinez, R.F., Yi, T., Villalona, G., Shinoka, T., *et al.* Tissue-engineered vascular grafts: does cell seeding matter? J Pediatr Surg **45,** 1299, 2010.
11. Wang, C., Cen, L., Yin, S., Liu, Q., Liu, W., Cao, Y., *et al.* A small diameter elastic blood vessel wall prepared under pulsatile conditions from polyglycolic acid mesh and smooth muscle cells differentiated from adipose-derived stem cells. Biomaterials **31,** 621, 2010.
12. Gauvin, R., Guillemette, M., Galbraith, T., Bourget, J.M., Larouche, D., Marcoux, H., *et al.* Mechanical properties of tissue-engineered vascular constructs produced using arterial or venous cells. Tissue Eng Part A **17,** 2049, 2011.
13. Hoerstrup, S.P., Zünd, G., Sodian, R., Schnell, A.M., Grünenfelder, J., and Turina, M.I. Tissue engineering of small caliber vascular grafts. Eur J Cardiothorac Surg **20,** 164, 2001.
14. Nerem, R.M. Role of mechanics in vascular tissue engineering. Biorheology **40,** 281, 2003.
15. Engelmayr, G.C., Soletti, L., Vigmostad, S.C., Budilarto, S.G., Federspiel, W.J., Chandran, K.B., *et al.* A novel flex-stretch-flow bioreactor for the study of engineered heart valve tissue mechanobiology. Ann Biomed Eng **36,** 700, 2008.
16. Trubel, W., Schima, H., Moritz, A., Raderer, F., Windisch, A., Ullrich, R., *et al.* Compliance mismatch and formation of distal anastomotic intimal hyperplasia in externally stiffened and lumen-adapted venous grafts. Eur J Vasc Endovasc Surg **10,** 415, 1995.
17. Billiar, K.L., and Sacks, M.S. Biaxial mechanical properties of the natural and glutaraldehyde treated aortic valve cusp-part I: experimental results. J Biomech Eng **122,** 23, 2000.
18. Tong, J., Cohnert, T., Regitnig, P., and Holzapfel, G.A. Effects of age on the elastic properties of the intraluminal thrombus and the thrombus-covered wall in abdominal aortic aneurysms: biaxial extension behaviour and material modelling. Eur J Vasc Endovasc Surg **42,** 207, 2011.
19. Waldman, S.D., Sacks, S.M., and Lee, J.M. Boundary conditions during biaxial testing of planar connective tissues Part II. J Mater Sci Lett **21,** 1215, 2002.
20. Sun, W., Sacks, S.M., and Scott, M. J. Effects of boundary conditions on the estimation of the planar biaxial mechanical properties of soft tissues. J Biomech Eng **127,** 709, 2005.
21. Ogden, R.W. Non-Linear Elastic Deformations. New edition ed. New York: Dover Publications, 1997.
22. Hollenstein, M., Ehret, A., Itskov, M., and Mazza, E. A novel experimental procedure based on pure shear testing of dermatome-cut samples applied to porcine skin. Biomech Modeling Mechanobiol **10,** 651, 2011.
23. Ehret, A., Hollenstein, M., Mazza, E., and Itskov, M. Porcine dermis in uniaxial cyclic loading: sample preparation, experimental results and modeling. J Mech Mater Struct. **6,** 1125, 2011.
24. Jabareen, M., Mallik, A.S., Bilic, G., Zisch, A.H., and Mazza, E. Relation between mechanical properties and microstructure of human fetal membranes: an attempt towards a quantitative analysis. Eur J Obstet Gynecol Reprod Biol **144,** S134, 2009.
25. Wells, S.M., Langille, B.L., Lee, J.M., and Adamson, S.L. Determinants of mechanical properties in the developing ovine thoracic aorta. Am J Physiol Heart Circ Physiol **277,** H1385, 1999.
26. Lally, C., Reid, A.J., and Prendergast, P.J. Elastic behavior of porcine coronary artery tissue under uniaxial and equibiaxial tension. Ann Biomed Eng **32,** 1355, 2004.
27. Vorp, D.A., Schiro, B.J., Ehrlich, M.P., Juvonen, T.S., Ergin, M.A., and Griffith, B.P. Effect of aneurysm on the tensile strength and biomechanical behavior of the ascending thoracic aorta. Ann Thorac Surg **75,** 1210, 2003.
28. Groenink, M., Langerak, S.E., Vanbavel, E., van der Wall, E.E., Mulder, B.J.M., van der Wal, A.C., *et al.* The influence of aging and aortic stiffness on permanent dilation and breaking stress of the thoracic descending aorta. Cardiovasc Res **43,** 471, 1999.
29. Gournier, J.P., Adham, M., Favre, J.P., Raba, M., Bancel, B., Lepetit, J.C., *et al.* Cryopreserved arterial homografts: preliminary study. Ann Vasc Surg **7,** 503, 1993.
30. Guinea, G.V., Atienza, J.M., Rojo, F.J., García-Herrera, C.M., Yiqun, L., Claes, E., *et al.* Factors influencing the mechanical behaviour of healthy human descending thoracic aorta. Physiol Meas **31,** 1553, 2010.
31. Duprey, A., Khanafer, K., Schlicht, M., Avril, S., Williams, D., and Berguer, R. *In vitro* characterisation of physiological and maximum elastic modulus of ascending thoracic aortic aneurysms using uniaxial tensile testing. Eur J Vasc Endovasc Surg **39,** 700, 2010.
32. Lokshin, O., and Lanir, Y. Micro and macro rheology of planar tissues. Biomaterials **30,** 3118, 2009.
33. Holzapfel, G., Gasser, T., and Ogden, R. A new constitutive framework for arterial wall mechanics and a comparative study of material models. J Elasticity **61,** 1, 2000.
34. Sacks, M.S. Incorporation of experimentally-derived fiber orientation into a structural constitutive model for planar collagenous tissues. J Biomech Eng **125,** 280, 2003.
35. Hariton, I., deBotton, G., Gasser, T., and Holzapfel, G. Stress-driven collagen fiber remodeling in arterial walls. Biomech Modeling Mechanobiol **6,** 163, 2007.
36. Baaijens, F., Bouten, C., and Driessen, N. Modeling collagen remodeling. J Biomech **43,** 166, 2010.
37. Cox RH. Passive mechanics and connective tissue composition of canine arteries. Am J Physiol Heart Circ Physiol **234,** H533, 1978.
38. Balguid, A., Mol, A., van Marion, M.H., Bank, R.A., Bouten, C.V.C., and Baaijens, F.P.T. Tailoring fiber diameter in electrospun poly(ε-caprolactone) scaffolds for optimal cellular infiltration in cardiovascular tissue engineering. Tissue Eng Part A **15,** 437, 2009.
39. Boerboom, R., Rubbens, M., Driessen, N., Bouten, C., and Baaijens, F. Effect of strain magnitude on the tissue properties of engineered cardiovascular constructs. Ann Biomed Eng **36,** 244, 2008.
40. Iwasaki, K., Kojima, K., Kodama, S., Paz, A.C., Chambers, M., Umezu, M., *et al.* Bioengineered three-layered robust and elastic artery using hemodynamically-equivalent pulsatile bioreactor. Circulation **118,** S52, 2008.
41. van Geemen, D., Vis, P.W., Soekhradj-Soechit, S., Sluijter, J.P.G., Beest, M., Kluin, J., *et al.* Decreased mechanical properties of heart valve tissue constructs cultured in platelet lysate as compared to fetal bovine serum. Tissue Eng Part C Methods **17,** 607, 2011.
42. Dahl, S., Rhim, C., Song, Y., and Niklason, L. Mechanical properties and compositions of tissue engineered and native arteries. Ann Biomed Eng **35,** 348, 2007.
43. Niklason, L.E., Gao, J., Abbott, W.M., Hirschi, K.K., Houser, S., Marini, R., *et al.* Functional arteries grown *in vitro*. Science **284,** 489, 1999.
44. Mohan, D., and Melvin, J.W. Failure properties of passive human aortic tissue. I–Uniaxial tension tests. J Biomech **15,** 887, 1982.

45. Stemper, B.D., Yoganandan, N., Stineman, M.R., Gennarelli, T.A., Baisden, J.L., and Pintar, F.A. Mechanics of fresh, refrigerated, and frozen arterial tissue. J Surg Res **139,** 236, 2007.
46. Vorp, D.A., Raghavan, M.L., Muluk, S.C., Makaroun, M.S., Steed, D.L., Shapiro, R., *et al.* Wall strength and stiffness of aneurysmal and nonaneurysmal abdominal aorta. Ann N Y Acad Sci **800,** 274, 1996.
47. Blondel, W.C.P.M., Lehalle, B., Maurice, G., Wang, X., and Stoltz, J.F. Rheological properties of fresh and cryopreserved human arteries tested *in vitro*. Rheologica Acta **39,** 461, 2000.
48. Konig, G., McAllister, T.N., Dusserre, N., Garrido, S.A., Iyican, C., Marini, A., *et al.* Mechanical properties of completely autologous human tissue engineered blood vessels compared to human saphenous vein and mammary artery. Biomaterials **30,** 1542, 2009.
49. L'Heureux, N., Pâquet, S., Labbé, R., Germain, L., and Auger, F.A. A completely biological tissue-engineered human blood vessel. FASEB J **12,** 47, 1998.
50. L'Heureux, N., Dusserre, N., Konig, G., Victor, B., Keire, P., Wight, T.N., *et al.* Human tissue-engineered blood vessels for adult arterial revascularization. Nat Med **12,** 361, 2006.

Address correspondence to:
Arabella Mauri, MSc
Department of Mechanical and Process Engineering
ETH Zurich
Center of Mechanics
Tannenstrasse 3
Zurich 8092
Switzerland

E-mail: mauri@imes.mavt.ethz.ch

Received: February 7, 2012
Accepted: September 21, 2012
Online Publication Date: January 2, 2013